Int Ophthalmol (2019) 39:829–837
https://doi.org/10.1007/s10792-018-0882-6

ORIGINAL PAPER

# Anterior segment ultrasound biomicroscopy image analysis using ImageJ software: Intra-observer repeatability and inter-observer agreement

**Azam Qureshi · Haoxing Chen · Osamah Saeedi · Mona A. Kaleem · Gianna Stoleru · Jordan Margo · Sachin Kalarn · Janet L. Alexander**

Received: 16 August 2017 / Accepted: 22 February 2018 / Published online: 7 March 2018


**Abstract**

*Purpose* In this novel study, we demonstrate a standardized imaging and measurement protocol of anterior segment (AS) structures with reliability analysis using ultrasound biomicroscopy (UBM) and ImageJ software.

*Methods* Ten pediatric and young adult patients undergoing examination under anesthesia for AS pathology were imaged using UBM. Four trained observers analyzed 20 images using ImageJ. Forty-five structural parameters were measured. Those that relied on the trabecular-iris angle (TIA) as a reference landmark were labeled TIA-dependent (TD) and all others were labeled non-TIA dependent (NTD). Intra-observer repeatability (IOR) and inter-observer agreement (IOA) of measurements were determined using coefficient of variation (CV) and intra-class correlation (ICC) followed by assessment of Bland–Altman plots (BAP) for each pair of observers, respectively.

*Results* For NTD parameters, non-ciliary body (CB) related measurements showed CV range 0.60–16.22% and ICC range 0.84–0.89, whereas CB-related parameters showed CV range 2.86–23.40% and ICC range 0.29–0.92. For TD parameters, parameters $< 2$ degrees removed from reference showed CV range 0.02–5.40% and ICC range 0.89–1.00, whereas parameters $> 1$ degree removed showed CV range 0.63–27.44% and ICC range 0.22–1.00. No systematic proportional bias was detected by BAPs.

*Conclusions* Preplaced landmarks yielded good IOR and IOA in quantitative assessment of AS structures that were NTD and non-CB-related or less removed from the reference. CB-related NTD measurements varied greatly in IOR and IOA, indicating protocol modifications or CB qualitative assessments needed to improve accuracy. Variability in TD measurements increased the further removed from the reference, which supports implementation of a reliable reference landmark to minimize variation.

**Keywords** UBM · Ultrasound biomicroscopy · Anterior segment · Pediatric · Congenital cataracts · Congenital glaucoma

**Electronic supplementary material** The online version of this article (https://doi.org/10.1007/s10792-018-0882-6) contains supplementary material, which is available to authorized users.

A. Qureshi (✉) · G. Stoleru
University of Maryland School of Medicine, Baltimore, MD, USA
e-mail: azam.qureshi@som.umaryland.edu

H. Chen
University Hospitals Case Medical Center, Cleveland, OH, USA

O. Saeedi · M. A. Kaleem · J. Margo · J. L. Alexander
University of Maryland Eye Associates, Baltimore, MD, USA

O. Saeedi · M. A. Kaleem · J. Margo · S. Kalarn · J. L. Alexander
Department of Ophthalmology, University of Maryland, Baltimore, MD, USA

## Introduction

Ultrasound Biomicroscopy (UBM) is commonly used by ophthalmologists to evaluate the anterior segment (AS) when investigating pathological mechanisms, disease course, and treatment responsiveness in many ocular diseases including cataracts and glaucoma [1–6]. The first practical UBM system was developed by Pavlin and Foster in 1990s [7]. UBM complements the traditionally used ten Megahertz B-scanner probes. An advantage of this technology is better resolution at the compromise of decreased depth [7], which is ideal for AS imaging.

Previous studies have validated the use of UBM to measure AS structures in adults [8–11]. However, there is a scarcity of work assessing UBM measurement reliability based on a standardized measurement protocol. The previously developed and traditionally utilized measurements by Pavlin et al. necessitate a sequential manner for measuring parameters related to the trabecular-iris angle (TIA), first requiring identification of the scleral spur (SS). The SS is used as the initial reference landmark for these sequential measures [8], however, as cited in previous literature, the SS can be difficult to identify [12], further adding to measurement variability. Testing of the utility and validity of a standardized protocol to sequentially measure and identify reference landmarks is needed to understand the clinical utility of these measurements. The present study seeks to achieve this objective, while eliminating variability of landmark identification by using preplaced lines set by a single observer at the TIA which is the highest contrast, and thus the most identifiable, image landmark.

Tello et al. studied thirteen AS measurements with basic statistical analysis [13]. This study investigates 45 AS measurements and utilizes multiple statistical methods for determining intra-observer reliability (IOR) and inter-observer agreement (IOA). Furthermore, methodological differences in this study allow for isolation of variability associated with sequential measurements by eliminating variation due to reference landmark identification. This is the first work to describe a standardized imaging and measurement protocol with corresponding reliability analysis for the pediatric and young adult AS using UBM and ImageJ software.

## Methods

Ten pediatric and young adult patients (median age = 2.5 years) were scheduled for examination under anesthesia due to AS pathology (including cataract, glaucoma and dysgenesis). UBM imaging was performed on twenty eyes using the Aviso Ultrasound Platform A/B UBM with 50 MHz linear transducer (Quantel Medical, Bozeman, MT). The orientation of six distinct images that were obtained in each eye is shown in Fig. 1. All images were de-identified. Demographics listed in Table 1 convey the diversity of patients and eye pathologies included in the study and Online Resource 1 is a composite of all study patient images included.

Inclusion criteria for the study include diagnosis of current unilateral or bilateral congenital, infantile, or childhood glaucoma, and history of congenital or infantile cataract before age 18, including patients age 1 week to 25 years old. Patients with previous history of intraocular surgery other than cataract extraction, secondary insertion of intraocular lens or glaucoma surgery, or history of traumatic glaucoma/cataract were excluded. Exclusion criteria from the control group of eyes for the average parameter sub-analysis include eyes with history of trauma, injury, intraocular surgery, past or present ocular anomaly, or refractive error greater than 4 diopters.

Four trained observers of varying levels of ophthalmology experience (first year medical student, third year medical student, post-graduate research associate, and attending ophthalmologist) measured

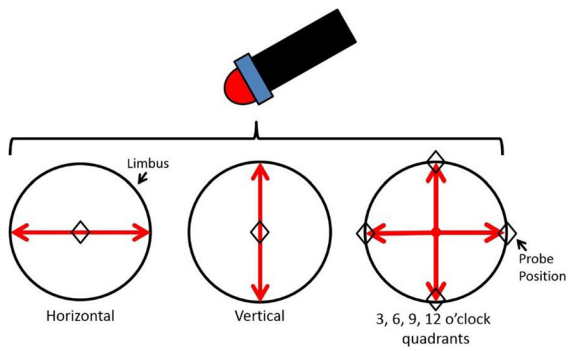


**Fig. 1** UBM probe orientation for six distinct images per patient eye. The black diamond denotes the location and centration of focus for each type of scan. The black circle illustrates the corneal limbus (Figure was created using Microsoft PowerPoint and Paint)

**Table 1** Patient demographics and pathology

| | Gender | Ethnicity | Eye | Pathology | Age | Syndrome |
|---|---|---|---|---|---|---|
| 1 | M | AA | Right | Preoperative cataract, pre-glaucoma | 5 weeks | Lowe |
| | | | Left | Pseudophakic, post-glaucoma surgery and sulcus tube | 7 months | |
| 2 | F | AA | Right | Preoperative Peters anomaly type I (iridocorneal adhesions, no lens involvement) | 1 week | Peters Plus |
| | | | Left | Preoperative Peters anomaly type I (iridocorneal adhesions, no lens involvement) | 1 week | |
| 3 | M | Nigerian | Right | Post-glaucoma surgery and AC tube | 22 months | None |
| | | | Left | Post-glaucoma angle surgery | 22 months | |
| 4 | M | AA | Right | Preoperative cataract | 4 years | None |
| | | | Left | Preoperative cataract | 4 years | |
| 5 | M | AA | Right | Preoperative cataract | 4 years 3 months | None |
| | | | Left | Aphakic, post-cataract surgery | 4 years 3 months | |
| 6 | M | AA | Right | Preoperative cataract | 2 months | Premature |
| | | | Left | None | 2 months | |
| 7 | F | AA | Right | None | 20 months | Premature |
| | | | Left | Preoperative cataract | 20 months | |
| 8 | M | Caucasian | Right | Preoperative cataract | 2 years | Trisomy 21 |
| | | | Left | Pseudophakic, post-cataract surgery | 2 years | |
| 9 | M | Caucasian | Right | Preoperative cataract | 23 years | Trisomy 21 |
| | | | Left | Preoperative cataract | 23 years | |
| 10 | F | Hispanic | Right | Pseudophakic, post-cataract surgery | 5 years 2 months | Trisomy 21 |
| | | | Left | Pseudophakic, post-cataract surgery | 5 years 2 months | |

*AA* African American

45 structural parameters in each image twice using ImageJ 1.48v (National Institutes of Health, Bethesda, MD, USA) (Table 2, Online Resource 2). ImageJ, an open-source software written in Java, allowed for observer-dependent measurements.

Measurements of TIA-dependent (TD) parameters required other reference lines/measurements to be taken first and were classified as a certain degree removed from the reference, which was a preplaced line at the TIA. The TIA was used as a landmark reference due to previous reports of scleral spur identification being unreliable [12]. Use of a preplaced line by a single observer on all images eliminated variability of locating the reference landmark, thereby isolating measurement variability following the protocol. Figure 2 illustrates the preplaced reference line segment for consistency.

All parameters were measured twice sequentially by resetting the image between the two sets of measurements. Ambiguous parameters were omitted in certain images due to image quality or pathological anatomy.

A comparison was carried out between group averages of each parameter from our study patient measurements (obtained by a single observer's single full set of observations) with measurements from 10 eyes of 10 control patients matched by age and ethnicity (Online Resource 3).

In the manner previously described, each control patient's eye was imaged 2–3 times (consisting of 2 of the previously described orientations, along with a dedicated cornea image in some cases). Each of the 27 total control patient images was measured once by a single observer.

Statistical analysis was performed to evaluate IOR and IOA using MedCalc (Windows version 15.6, MedCalc Software, Ostend, Belgium). IOR was determined by calculating the CV, while also determining the repeatability coefficient ($r$) for each parameter. IOA was analyzed by computing the ICC for all observers and Bland–Altman Plot (BAP)

**Table 2** List of 45 measured parameters with clinical significance with ophthalmic pathology

| Measurement | Description adapted to present protocol |
|---|---|
| CCT | Inner endothelium to outer epithelium of central cornea [1] |
| ParaCT[a] | Inner endothelium to outer epithelium of cornea 45° off-center. Distinct from central and peripheral corneal thickness [15] |
| AC Depth | Measured from inner corneal endothelium to outer surface of the anterior central lens capsule (or approximated central lens position for aphakic eyes) [1, 2, 8, 14, 16] |
| Pupil Size | Distance between central-most points of irises [17] |
| SR Area[a] | Area within boundaries of SR [5] |
| SR Integrated Density[a] | Calculated by ImageJ (Area × Mean Gray Value), surrogate for tissue density [5] |
| SS Distance | Length between sulcus angle apices [11] |
| AA Distance | Length between TIA apices [18, 19] |
| TCPD[a] | Length from inner corneal endothelium point 500 μm from TIA apex to the anterior ciliary process, measured perpendicular to iris [2, 8, 14] |
| ID1[a] | Iris thickness along TCPD line [2, 8] |
| ID2[a] | Iris thickness at 2 mm from iris root [1, 2, 8] |
| ID3[a] | Iris thickness between ID2 and central tip of iris [1, 2, 8] |
| AOD500[a] | Perpendicular length from inner corneal endothelium point 500 μm from TIA apex to outer surface of iris at a point [2, 4, 8, 16] |
| CB Length[a] | Length of CB measured along CB midline [3] |
| CB Thickness[a] | Thickness of CB measured at point halfway along its length [10] |
| CB Area[a] | Area within boundaries of CB [3, 6, 20] |
| CB Integrated Density[a] | Calculated by ImageJ (Area × Mean Gray Value) and considered as marker for tissue density [6, 20] |
| CICD[a] | Length along which CB is in contact with iris |
| ILCD[a] | Length along which lens is in contact with iris [2, 8, 21] |
| ICPD[a] | Length from inner iris surface to outer CB boundary (measured along TCPD line) [21] |
| Theta 1[a] | Angle measured between point 500 μm from TIA apex along inner corneal endothelium and point where AOD500 meets the iris, with an apex at the TIA [8, 16]. Relevant to iris base position |
| Theta 2[a] | Angle measured between points along lens and along iris 500 μm from the peripheral-most point of contact between lens and iris. Relevant to lens position [8] |
| Theta 3[a] | Angle measured between iris midline and 500 μm line from TIA apex along inner corneal endothelium. Relevant to overall iris position [8] |
| Theta 4[a] | Angle measured between CB midline and 500 μm line from TIA apex along inner corneal endothelium. Relevant to overall CB position [8] |
| Theta 5[a] | Angle measured between inner surface of iris and outer boundary of CB. Relevant to CB base position [3, 10, 14] |

*CCT* central corneal thickness, *ParaCT* paracentral corneal thickness, *AC* anterior chamber, *SR* Soemmering Ring, *SS* sulcus-to-sulcus, *AA* angle-to-angle, *TCPD* trabecular-ciliary process distance, *ID* iris thickness, *AOD* angle opening distance, *CB* ciliary body, *CICD* ciliary body contact distance, *ILPD* iris-lens contact distance, *ICPD* iris-ciliary process distance

[a]Parameter exists on both the left and right side of the image on the same eye

analysis for each pair of observers. Comparison between average parameters from study patients and control patients was carried out by implementing the exact Wilcoxon test using SAS 9.3 (SAS Institute Inc., Cary, NC, USA). $p$ values less than 0.05 were considered statistically significant.

## Results

Parameters were divided into NTD or TD parameters based on whether the measurement required the TIA reference. TD parameters were characterized into degrees removed from reference based on number of

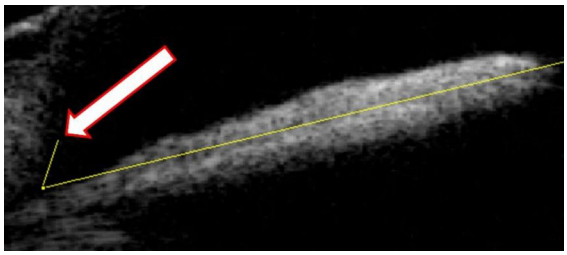

**Fig. 2** Arrow points to preplaced reference line that starts 500 μm from the apex of the trabecular-iris angle (TIA) and running along the inner corneal endothelium and across the iris plane. This line was placed on every distinguishable TIA by the same observer to ensure consistency (Figure was created using an UBM image captured using Aviso Ultrasound Platform A/B UBM, Image J, and edited using Microsoft PowerPoint and Paint)

reference lines/measurements required by the protocol from the initial TIA landmark to obtain the designated parameter. Anterior chamber depth (ACD) is shown in Fig. 3 as an example.

Table 4 presents IOR results for TD measures. There is greater variability of measurements further removed from the preplaced lines. For TD parameters, parameters $< 2$ degrees removed from reference showed CV range 0.02–5.40%, whereas parameters $> 1$ degree removed showed CV range 0.63–27.44% (Table 4).

Non-CB-related measurements showed CV range 0.02–16.22% (Tables 3, 4), whereas CB-related parameters showed CV range 1.77–27.44% (Tables 3, 4).

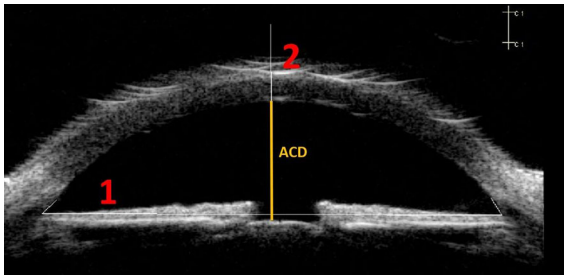


**Fig. 3** ACD is an example of a TD parameter. ACD was measured from the inner corneal endothelium to the outer surface of the lens along a perpendicular bisector of a line connecting the TIA apices. Before the measurement could be made (1) a line connecting the TIA angle apices was needed, followed by (2) a perpendicular bisector (along which the ACD measurement was made). Therefore, ACD was considered 2 degrees removed from the TIA apex (Figure was created using an UBM image captured using Aviso Ultrasound Platform A/B UBM, Image J, and edited using Microsoft PowerPoint and Paint)

Table 5 presents IOA results for NTD measures. Poor agreement (overall ICC $< 0.7$) in all parameters describing ciliary body position is consistent with the suggested reduced repeatability for CB-related parameters (Tables 3, 4).

For NTD parameters, non-CB-related measurements showed ICC range 0.84–0.89, whereas CB-related parameters showed ICC range 0.29–0.92. For TD parameters, parameters $< 2$ degrees removed from reference showed ICC range 0.89–1.00, whereas parameters $> 1$ degree removed showed ICC range 0.22–1.00. BAP's demonstrated no variation in reliability related specifically to measurements' underlying values (data not shown). Overall, 52% (12/23) of the measured parameters demonstrated an ICC $> 0.7$. For 17% (4/23) of parameters, agreement was found to be very poor with ICC $< 0.4$. The trend in IOA for less agreement of measures further removed from the preplaced lines resembles that observed in IOR analysis (Table 6).

Average overall parameters from study patients were compared to those in age- and ethnicity-matched control patients. Only AA distance yielded a significant difference between control eyes and study eyes ($p = 0.023$, Table 7). No significant differences were found for any parameter (Table 7).

## Discussion

The configuration of the AS is important for understanding pathological mechanisms, disease course, and treatment responsiveness in many ocular diseases. This study clarifies the reliability and repeatability of systematic measurements using our protocol, while conveying which parameters can be reliably measured using ImageJ software. This information allows for a better understanding of past and future UBM image analysis studies.

IOR and IOA results conveyed low reliability of measurements related to the CB. This finding can be explained by the fact that the CB is deeper in the AS compared to other parameters, and image resolution decreases with further distance from the UBM probe. Qualitative assessment of the CB and dedicated CB images would improve accuracy and consistency of CB-related measurements. Two-dimensional imaging

**Table 3** IOR results for NTD measures

| Measurement | CV range | *r* range |
|---|---|---|
| Pupil size | 2.23–3.35 | 95.22–142.80 μm |
| SS distance | 0.60–2.23 | 154.36–609.74 μm |
| CB length | 1.77–10.12 | 105.60–687.17 μm |
| CB thickness | 3.99–8.11 | 72.05–166.61 μm |
| CB area | 2.86–7.36 | 126,456.35–320,312.22 $\mu m^2$ |
| CB integrated density | 3.05–9.60 | 13.51–31.84 U |
| CICD | 5.44–13.55 | 155.38–468.70 μm |
| ILCD | 3.14–7.31 | 111.35–261.14 μm |
| Theta 2 | 10.05–16.22 | 4.34°–9.18° |
| Theta 5 | 11.28–23.40 | 8.84°–12.24° |

**Table 4** IOR results for TD measures

| Measurement | Degrees removed from reference | CV range | R range |
|---|---|---|---|
| AA distance | 0 | 0.02-0.14 | 7.02 – 42.36 μm |
| AOD500 | 1 | 1.41-5.06 | 21.61 – 74.19 μm |
| Theta 1 | | 1.55-5.40 | 1.9° – 6.14° |
| TCPD | | 1.44-3.26 | 29.89 – 67.19 μm |
| CCT | 2 | 3.42-4.73 | 56.17 – 87.77 μm |
| ACD | | 0.63-1.47 | 42.05 – 101.55 μm |
| ICPD | | 9.42-27.44 | 37.64 – 74.72 μm |
| ID1 | | 4.75-8.73 | 32.89 – 51.18 μm |
| ID2 | | 3.68-5.51 | 39.01 – 53.84 μm |
| Theta 3 | | 1.91-2.77 | 2.37° – 3.37° |
| Theta 4 | | 3.30-6.16 | 4.31° – 9.97° |
| ID3 | 3 | 4.31-5.45 | 55.93 – 78.15 μm |
| ParaCT | 4 | 3.06-12.01 | 51.39 – 232.65 μm |

Darker colored rows indicate parameters further removed from the reference landmark

is of limited use when examining cross sections of individual ciliary processes. Because cross-sectional imaging may land on a single process or between processes, measurements are highly dependent upon image location (even if proven reliable). Transverse imaging along the row of ciliary processes using UBM may yield more useful information with respect to this particular ocular structure.

Decreasing IOR and IOA values of TD parameters with increasing degrees removed from the TIA reference line was predicted due to compounded subjectivity in the sequential measurement method. Preplaced reference lines yielded good IOR and IOA in quantitative assessment of AS structures that were NTD and non-CB related, or less removed from reference. The preplaced line helped to evaluate consistency of the protocol among observers by removing subjectivity of each individual identifying the reference landmark. Furthermore, the substitution of SS with TIA as the reference landmark contrasts Pavlin's initial methods of AS measurements [8]. The SS is a difficult structure to accurately locate in the images. Using the SS as a reference potentially results in identification errors and variability among several observers which would compromise all dependent measurements. Indeed, previous work using AS optical coherence tomography has shown 72% confidence

**Table 5** IOA results for NTD measures

| Agreement | Measurement | Overall ICC, 95% CI | Number of images |
|---|---|---|---|
| Good | CB integrated density | 0.92, 0.79–0.97 | 14 |
| | SS distance | 0.89, 0.59–0.97 | 10 |
| | Pupil size | 0.88, 0.61–0.96 | 17 |
| | ILCD | 0.85, 0.54–0.96 | 12 |
| | Theta 2 | 0.84, 0.66–0.95 | 11 |
| Poor | CB Area | 0.65, 0.30–0.86 | 14 |
| | CB Thickness | 0.62, 0.35–0.84 | 14 |
| | CB Length | 0.49, 0.17–0.77 | 14 |
| | CICD | 0.48, 0.23–0.74 | 15 |
| | Theta 5 | 0.29, 0.07–0.58 | 17 |

All 5 of the parameters with poor agreement (overall ICC $< 0.7$) describe ciliary body position

**Table 6** IOA results for TD measures

| Measurement | Degrees removed from reference | ICC, 95% CI | Number of images |
|---|---|---|---|
| AA distance | 0 | 1.00, 0.99–1.00 | 12 |
| AOD500 | 1 | 0.98, 0.92–0.99 | 20 |
| TIA | | 0.96, 0.92–0.98 | 20 |
| TCPD | | 0.89, 0.77–0.96 | 15 |
| CCT | 2 | 0.72, 0.50–0.88 | 14 |
| ACD | | 1.00, 1.00–1.00 | 8 |
| ICPD | | 0.54, 0.22–0.80 | 15 |
| ID1 | | 0.22, 0.02–0.49 | 18 |
| ID2 | | 0.24, 0.04–0.53 | 16 |
| Theta 3 | | 0.99, 0.97–0.99 | 19 |
| Theta 4 | | 0.63, 0.33–0.85 | 14 |
| ID3 | 3 | 0.59, 0.23–0.83 | 16 |
| ParaCT | 4 | 0.25, 0.03–0.57 | 14 |

Darker colored rows indicate parameters further removed from the reference landmark

**Table 7** Results from comparison of average overall parameters in study patients to those in age- and ethnicity-matched control patients

| Comparison between study patients and age- and ethnicity-matched control patients | |
|---|---|
| Parameter | Statistical significance |
| CCT | NS ($p = 0.53$) |
| ParaCT | NS ($p = 0.32$) |
| ACD | NS ($p = 0.37$) |
| Pupil size | NS ($p = 0.58$) |
| AA distance | $p = 0.02$ |
| SS distance | NS ($p = 0.88$) |
| TCPD | NS ($p = 0.68$) |
| ID1 | NS ($p = 0.53$) |
| ID2 | NS ($p = 0.91$) |
| ID3 | NS ($p = 0.91$) |
| AOD500 | NS ($p = 0.58$) |
| CB length | NS ($p = 0.36$) |
| CB thickness | NS ($p = 0.78$) |
| CB area | NS ($p = 0.28$) |
| CB integrated density | NS ($p = 0.50$) |
| CICD | NS ($p = 0.55$) |
| ILCD | NS ($p = 0.39$) |
| ICPD | NS ($p = 0.85$) |
| Theta 1 | NS ($p = 0.63$) |
| Theta 2 | NS ($p = 0.45$) |
| Theta 3 | NS ($p = 0.09$) |
| Theta 4 | NS ($p = 0.84$) |
| Theta 5 | NS ($p = 0.07$) |

Only AA distance discrepancies between control and study groups reached statistical significance

*NS* not significant

in SS location [12]. The TIA is a significantly less ambiguous location, primarily due to the fact that this angle occurs at a fluid-tissue interface that is well-resolved with ultrasound. The SS is at a tissue–tissue interface, yielding less contrast. This study shows increased measurement variation in TD measurements increasingly removed from the reference landmark, despite the reference being placed by a single observer. With different observers using his or her own judgement in identification of the SS, this variation would be expected to increase even more. Results of our study confirm the necessity of using a more reliable landmark than the SS for AS TD measurements in order to minimize measurement variation.

Many studies have published quantitative assessments of AS UBM imaging to help understand changes that occur as a result of treatment or disease [1, 2, 4, 14]. For example, CCT is larger in infants with primary congenital glaucoma in comparison with controls [1] and ACD deepens after cataract surgery [14]. Our results put previous findings in context by showing that multiple anterior chamber parameters can be reliably measured from UBM images using ImageJ software. Excluding structures with unreliable measurements should be strongly considered when planning future prospective analysis of AS measurements using UBM and ImageJ.

Limitations of this study include the (1) the lack of insight on the accuracy of UBM measurements, (2) lack of analysis on normal eyes, (3) possible bias from limited ethnic diversity, and (4) no corresponding analysis using a preplaced line at the SS for comparison. First, our results on reliability and repeatability do not speak to the accuracy of any measurements or the accuracy of the preplaced landmark. Gold-standard methods of measurement for comparison do not exist for all measured parameters in this study. In order to maximize accuracy, observers were instructed to only make measurements where image quality provided discernable structures. Second, our analysis did not include a sufficient number of normal eyes (N = 2) to allow for any comparison in measurement variability between images of normal eyes and images of eyes with pathology. Furthermore, 7 of the 10 study patients were of African descent, suggesting a possible bias in the sample. Indeed, evidence suggests that small variability in AS structure occurs between different ethnic groups [22–24]. However, patients in

our sample represent a wide diversity of ages and eye pathologies, with representation of both males and females in pre- and postoperative states (Table 1), thereby contributing to provide a robust testing of IOR and IOA overshadowing any slight bias in measurements conferred by a study sample limited in ethnic variation. Our results likely still overestimate the variability associated with AS UBM image measurements of the general population of pediatric and young adult eyes without pathology. This hypothesized discrepancy could arise from better defined structures and/or differing magnitudes of parameter measurements in patients without eye pathology. To address these possible concerns, we convey that our BAP analysis (data not shown) did not suggest any reliability variation based on the magnitude of measures, and further, a comparison of our study data to a sample of age- and ethnicity-matched control eyes conveys significant difference in the magnitude of average AA distance, but no other parameter examined. This combination of findings supports the external validity of our data to patients lacking eye pathology. Lastly, we did not analyze images with a preplaced line at the SS in order to investigate whether or not our starting point definitively leads to any less discrepancy in measurement reliability in comparison with the reliability of measurements made using the more ambiguously determined SS. However, because the lines are preplaced, landmark identification would not factor into any discrepancy, which would likely be negligible.

Despite a small sample size, our selection of cases covers all of the most common AS diseases in children, including cataract, glaucoma, and AS dysgenesis, while providing pre- and postoperative status for these diseases. Our demographics include various ages, male and female genders, and a representation of multiple ethnicities, including African, Caucasian, and Hispanic. In our presentation of such a heterogeneous group of cases, with subsequent comparison with control eyes, we have established that our protocol can be broadly applied to the majority of pediatric and adult patients. Although evidence suggests that variability in AS structure occurs between different ages of patients, different demographic groups, different ocular pathologies, and results in alterations from surgical manipulations, investigation into these differences are beyond the scope of this work, which aims to demonstrate a reliable and reproducible protocol for the systematic and quantitative evaluation of a variety of UBM images [22–28].

The reliability assessment provided by this study is widely relevant in understanding the clinical utility of these and other AS UBM measurement studies. The long-term goal of our study is to produce a database of AS measurements in diverse pediatric and young adult patients with longitudinal postoperative follow-up to evaluate the relationships between AS parameters in congenital ophthalmic diseases, clinical outcomes related to visual function, and risk profile of associated complications.

**Acknowledgements** This work was supported by: (1) The Knights Templar Eye Foundation Career Starter Grants for 2015–2016 awarded to Dr. Janet Alexander and (2) The K23 Career Development Award from the National Eye Institute (K23EY025014) awarded to Dr. Osamah Saeedi. We would like to acknowledge Cierra McKoy for contributing to this work.

**Compliance with ethical standards**

**Conflict of interest** No authors report conflict of interest.

**Ethical approval** All procedures performed were in accordance with the ethical standards of the institutional and/or national research committee and with the 1964 Helsinki Declaration and its later amendments or comparable ethical standards. No animals were included in this study.

**Informed consent** This work involved human participants in which appropriate informed consent was obtained.

## References

1. Hussein TR, Shalaby SM, Elbakary MA, Elseht RM, Gad RE (2014) Ultrasound biomicroscopy as a diagnostic tool in infants with primary congenital glaucoma. Clin Ophthalmol (Auckland, NZ) 8:1725
2. Mérula RV, Cronemberger S, Diniz Filho A, Calixto N (2008) New comparative ultrasound biomicroscopic findings between fellow eyes of acute angle closure and glaucomatous eyes with narrow angle. Arquivos Brasileiros de Oftalmologia 71(6):793–798
3. Prata TS, Dorairaj S, De Moraes CG et al (2013) Is preoperative ciliary body and iris anatomical configuration a predictor of malignant glaucoma development? Clin Exp Ophthalmol 41(6):541–545
4. Pavlin CJ, Harasiewicz K, Foster FS (1992) Ultrasound biomicroscopy of anterior segment structures in normal and glaucomatous eyes. Am J Ophthalmol 113(4):381–389
5. Kobayashi H, Hirose M, Kobayashi K (2000) Ultrasound biomicroscopic analysis of pseudophakic pupillary block

glaucoma induced by Soemmering's ring. Br J Ophthalmol 84(10):1142–1146
6. Marigo FA, Finger PT, McCormick SA et al (2000) Iris and ciliary body melanomas: ultrasound biomicroscopy with histopathologic correlation. Arch Ophthalmol 118(11):1515–1521
7. Pavlin CJ, Harasiewicz K, Sherar MD, Foster FS (1991) Clinical use of ultrasound biomicroscopy. Ophthalmology 98(3):287–295
8. Pavlin CJ, Foster FS (1992) Ultrasound biomicroscopy in glaucoma. Acta Ophthalmol 70(S204):7–9
9. Dada T, Sihota R, Gadia R, Aggarwal A, Mandal S, Gupta V (2007) Comparison of anterior segment optical coherence tomography and ultrasound biomicroscopy for assessment of the anterior segment. J Cataract Refract Surg 33(5):837–840
10. Wang Z, Huang J, Lin J, Liang X, Cai X, Ge J (2014) Quantitative measurements of the ciliary body in eyes with malignant glaucoma after trabeculectomy using ultrasound biomicroscopy. Ophthalmology 121(4):862–869
11. Oh J, Shin HH, Kim JH, Kim HM, Song JS (2007) Direct measurement of the ciliary sulcus diameter by 35-megahertz ultrasound biomicroscopy. Ophthalmology 114(9):1685–1688
12. Narayanaswamy A, Sakata LM, He MG et al (2010) Diagnostic performance of anterior chamber angle measurements for detecting eyes with narrow angles: an anterior segment OCT study. Arch Ophthalmol 128(10):1321–1327
13. Tello C, Liebmann J, Potash SD, Cohen H, Ritch R (1994) Measurement of ultrasound biomicroscopy images: intraobserver and interobserver reliability. Invest Ophthalmol Vis Sci 35(9):3549–3552
14. Nonaka A, Kondo T, Kikuchi M et al (2006) Angle widening and alteration of ciliary process configuration after cataract surgery for primary angle closure. Ophthalmology 113(3):437–441
15. Feizi S, Jafarinasab MR, Karimian F, Hasanpour H, Masudi A (2014) Central and peripheral corneal thickness measurement in normal and keratoconic eyes using three corneal pachymeters. J Ophthalmic Vis Res 9(3):296–304. https://doi.org/10.4103/2008-322x.143356
16. Kurimoto Y, Park M, Sakaue H, Kondo T (1997) Changes in the anterior chamber configuration after small-incision cataract surgery with posterior chamber intraocular lens implantation. Am J Ophthalmol 124(6):775–780
17. Kanellopoulos AJ, Asimellis G (2014) Clear-cornea cataract surgery: pupil size and shape changes, along with anterior chamber volume and depth changes. A Scheimpflug imaging study. Clin Ophthalmol (Auckland, NZ) 8:2141
18. Goldsmith JA, Li Y, Chalita MR, Westphal V, Patil CA, Rollins AM, Izatt JA, Huang D (2005) Anterior chamber width measurement by high-speed optical coherence tomography. Ophthalmology 112(2):238–244
19. Piñero DP, Plaza Puche AB, Alió JL (2008) Corneal diameter measurements by corneal topography and angle-to-angle measurements by optical coherence tomography: evaluation of equivalence. J Cataract Refract Surg 34(1):126–131. https://doi.org/10.1016/j.jcrs.2007.10.010
20. Chua J, Muen WJ, Reddy A, Brookes J (2012) The masquerades of a childhood ciliary body medulloepithelioma: a case of chronic uveitis, cataract, and secondary glaucoma. Case reports in ophthalmological medicine
21. Németh J, Csákány B, Pregun T (1996) Ultrasound biomicroscopic morphometry of the anterior eye segment before and after one drop of pilocarpine. Int Ophthalmol 20(1–3):39–42
22. Kobayashi H, Ono H, Kiryu J, Kobayashi K, Kondo T (1999) Ultrasound biomicroscopic measurement of development of anterior chamber angle. Br J Ophthalmol 83:559–562
23. Wang D, He M, Wu L, Yaplee S, Singh K, Lin S (2012) Differences in iris structural measurements among American Caucasians, American Chinese, and mainland Chinese. Clin Exp Ophthalmol 40(2):162–169
24. Lee RY, Huang G, Porco TC, Chen YC, He M, Lin SC (2013) Differences in iris thickness among African Americans, Caucasian Americans, Hispanic Americans, Chinese Americans, and Filipino-Americans. J Glaucoma 22(9):673–678
25. Leung CK, Palmiero PM, Weinreb RN, Li H, Sbeity Z, Dorairaj S, Leung D, Liu S, Liebmann LM, Congdon N, Lam DS, Ritch R (2010) Comparisons of anterior segment biometry between Chinese and Caucasians using anterior segment optical coherence tomography. Br J Ophthalmol 94(9):1184–1189
26. Mérula RV, Cronemberger S, Diniz Filho A, Calixto N (2008) New comparative ultrasound biomicroscopic findings between fellow eyes of acute angle closure and glaucomatous eyes with narrow angle. Arq Bras Oftalmol 71(6):793–798
27. Hussein TR, Shalaby SM, Elbakary MA, Elseht RM, Gad RE (2014) Ultrasound biomicroscopy as a diagnostic tool in infants with primary congenital glaucoma. Clin Ophthalmol (Auckland, NZ) 8:1725
28. Kanellopoulos AJ, Asimellis G (2014) Clear-cornea cataract surgery: pupil size and shape changes, along with anterior chamber volume and depth changes. A Scheimpflug imaging study. Clin Ophthalmol (Auckland, NZ) 8:2141